An evaluation on the clinical outcome prediction of rotor detection in non-invasive phase maps.

C. Fambuena-Santos[1], I. Hernández-Romero[2], R. Molero[1], A.M. Climent[1], M.S. Guillem[1]

[1]ITACA Institute, Universitat Politècnica de València, Valencia, Spain
[2]Department of Signal Theory and Communications, Universidad Rey Juan Carlos, Madrid, Spain

Abstract

Phase maps obtained from Electrocardiographic imaging (ECGI) have been used in the past for rotor identification and ablation guidance in atrial fibrillation (AF). In this study, we propose a new rotor detection algorithm and evaluate its potential use for prediction of pulmonary vein isolation (PVI) success.

The mean precision and recall of the algorithm were evaluated by using manually annotated ECGI phase maps and resulted in 0.82 and 0.75, respectively.

Phase singularities and rotors were then quantified on ECGI signals from 29 patients prior to PVI.

A significantly higher concentration of phase singularities (PSs) in the pulmonary veins in patients with a successful PVI was found. Our results suggest that rotor-related metrics obtained from ECGI derived phase maps contain relevant information to predict clinical outcome in PVI patients.

1. Introduction

In the last years, theories supporting well localized drivers as the cause of atrial fibrillation (AF) have gained relevance[1]. Rotors are a well described type of local driver consisting on rotational activation patterns that perpetuate asynchronous electrical propagation in the heart. A technology capable of identifying rotors is the electrocardiographic imaging (ECGI). ECGI is a non-invasive 3D mapping technology which projects the electrical activity registered on the torso of patients directly on the atria. The most extended methodology used nowadays to localize rotors using ECGI is based on phase singularities (PSs) detections from phase maps. Many strategies have been developed in the past to identify PSs automatically [2]. However, the lack of standardized preprocessing techniques prior to phase map generation, possible conditioning of these preprocessing operations on the resultant signal, and the high difficulty and cost associated to ECGI validation have raised skepticism on phase map accuracy and confusion about the electrophysiological interpretation of PSs [3,4].

In this study, a new ECGI rotor detection algorithm is presented and applied on real AF data with 2 main objectives: 1) Evaluate the use of different rotor metrics to predict the clinical outcome of patients undergoing PVI and 2) Provide new insights on how the PS obtained from phase maps can be electro-physiologically interpreted.

2. Material and Methods

2.1. Data Acquisition and Processing

Body Surface Potential Maps (BSPM) were recorded in 29 patients with AF right before pulmonary vein isolation (PVI) and during infusion of adenosine, which transiently stops the ventricular activity. A set of 57 electrodes were employed to record the signals. A total of 2 segments per patient with similar durations (4.06±0.311 s) were included in the database except for 1 subject for which only one segment could be used. The acquisition and preprocessing protocols employed in this study were already presented in [5]. As an overview, the inverse problem was calculated using zero order Tikhonov regularization and L-curve optimization. The geometry of the torso and electrode positions were determined using photogrammetry. The anatomy of the atria was segmented from MRI/CT images. Once the 3D voltage maps were obtained, these were transformed into 2D squared images following the procedure presented in [6]. Phase maps were then computed out of 2D voltage maps by means of the Hilbert transform.

Patients participating in this study were split into 2 groups attending to their outcome 6 months after PVI. Those that returned to sinus rhythm were labelled as 'Successful PVI' patients (n = 15) and those that presented any kind of arrhythmia (i.e. AF or Atrial flutter) were classified as 'Unsuccessful PVI' (n = 14). For validating the rotor-detection algorithm, a dataset of 9 segments where reentrant patterns could be visually identified were selected from the database. An application developed in MATLAB 2020 was used to manually label the location of

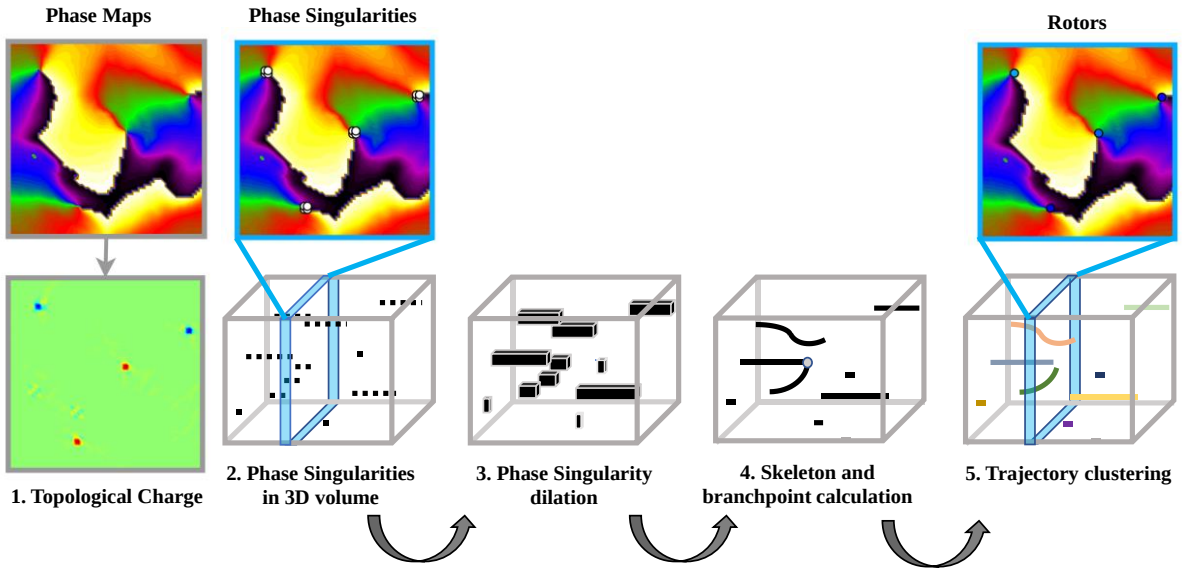

Figure 1. 3D operations applied in the rotor detection algorithm and correspondent views on phase maps: **1)** The topological charge is calculated out of the input phase maps using 3D convolution operations. **2)** A threshold is applied to obtain a binary 3D volume containing the space-temporal locations of phase singularities. **3)** 3D dilation is applied on this volume in order connect close phase singularities and conform the space-temporal trajectories of rotors**. 4)** Skeleton of dilated volume is calculated and branch points are detected in order to remove crossing points in the trajectories. **5)** Region growing is applied to the skeletonized volume in order to cluster the trajectories.

the PS found in the validation dataset.

2.2. Rotor Detection Algorithm

The workflow of the rotor detection algorithm is depicted in Figure 1. The input data for the proposed algorithm is a volume of instantaneous 2D phase maps stacked in the third dimension. The first step consists in detecting PSs in this volume using the topological charge method [2,7,8]. PSs with a non-linear phase progression in their surroundings were discarded. The remaining PS were then stored as a volume of binary images encoding their space-temporal locations. Then, 3D binary dilation was performed, which allows connecting neighbouring PS and fill the gaps produced by small misdetections. However, dilation may also connect non-related trajectories introducing crossing points. In order to identify these crossings, the dilated volume was skeletonized and branchpoints were detected. Branchpoints are positions in the volume where two or more different trajectories converge. Trajectories converging at branchpoints were split. Then, region growing was applied to classify them into different rotors. This classification was refined by checking the extremes of consecutive rotor trajectories and grouping them together when a pair of starting-ending points were close. Finally, the number of turns of each rotor was estimated by checking the temporal phase evolution around them.

2.3. Metrics and Statistical Analysis

The precision (P) and recall (R) of the algorithm were computed as the ratio between the number of true positive detections over all the detections, and the number of true positives detections over all the labelled PSs (true PSs). Only the rotors that spin for at least 1 turn were included in the validation analysis. Furthermore, the F_β score introduced in this study was also computed. This parameter summarizes the information of both, recall and precision and allows to weight their relevance in the final score through the parameter β (see equation 1). In this study a value of β = 2 was used.

$$F_\beta = (1+\beta^2)\cdot\frac{P\cdot R}{\beta^2\cdot P + R} \qquad (1)$$

Different rotor-related metrics were computed in AF patient's data: The number of rotors per second, the number of PSs in the PPVV per second, the number of PS in the whole atria per second and the ratio of PS in the PPVV over PSs in the rest of the atria. All these metrics where computed using two different sets of rotors. In the first one all the rotors detected by the proposed algorithm were included (0-turn rotors), while in the second only the rotors that spin for at least 1 turn (1-turn rotors) were considered. The Mann-Whitney U test was used in order to compare the value of the mentioned metrics in the 'Successful PVI' and 'Unsuccessful PVI' groups.

3. Results

3.1. Rotor detection Algorithm Validation

Table 1 presents the recall, precision and F-score values obtained in all the recordings conforming the validation dataset. The mean values of these parameters were 0.75, 0.82 and 0.75 respectively.

Recall	Precision	F-score
0.91	0.74	0.87
0.74	0.70	0.73
0.71	1.00	0.76
0.74	0.76	0.74
0.81	0.63	0.76
0.62	0.77	0.65
0.54	1.00	0.60
0.82	0.80	0.81
0.84	0.97	0.87

Table 1. Recall, Precision and F-score values obtained in the validation data set.

The mean number of PSs detected and manually labelled was compared at different regions (figure 2). As it can be observed, there was a very good correspondence between the annotated and automatically detected PSs, with errors ranging from 42 to 0 %. The region presenting the largest relative error was the left inferior pulmonary vein (LIPV) and the minimum was found in the right superior pulmonary vein (RSPV). The regions with higher number of labelled and detected PSs were the left and right atrial bodies (LB and RB) which are also significantly larger than the rest. LB presented also higher number of detected and labelled PSs than the RB region. Regarding the PPVV, both the right and left inferior PPVV (RIPV and LIPV) contained a significantly more PSs than the superior PPVV.

3.2. Rotor Metrics exploration in AF patients

No statistically significant differences were found in the number of PSs in the whole atria for patients with a successful vs unsuccessful PVI (figure 3B), although patients with an unsuccessful PVI had more connected PSs (rotors lasting for less than 1 turn, figure 3D): medians of 88.21 vs. 68.55 ($p<0.05$), but no differences were observed for the amount of rotors lasting more than 1 turn.

However, patients with a successful PVI presented more singularity points in the pulmonary vein area than those without a successful PVI (median of 26.28 vs. 12.16, $p<0.05$) and a higher ratio of the singularity points in the PV area with respect to the PSs in the rest of the atria (median of 0.16 vs. 0.04, $p<0.01$).

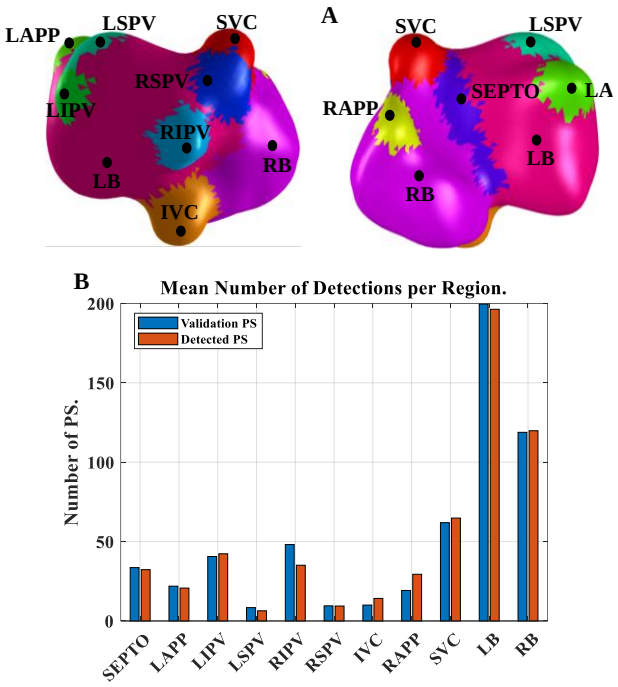

Figure 2. Results of the atrial segmentation and validation of the rotor detection algorithm: **A** show the front and back view of an example atrial model. **B** contains the mean number of PS per region of all the recordings used in the validation.

4. Discussion and Conclusions

This study presents a new method to detect PSs and cluster them into rotors using phase maps and ECGI. The precision and recall of the proposed algorithm were calculated using real AF data. Finally, a set of rotor metrics were computed and related to the clinical outcome of a set of AF patients treated with PVI.

The mean F-score obtained (0.75) is similar to other values already presented in the literature. In [2], 4 different rotor detection algorithms were evaluated using this score, which ranged between [0.527, 0.831] and they were all tested in 2D geometries. In our study, we present a novel method valid for 3D geometries and, therefore, applicable to a more general framework, by converting our data from a 3D geometry into a 2D space.

ECGI rotor-related metrics have already been evaluated to predict ablation outcome [9,5] but very few studies have reported on spatial dominance of the presence of these rotors and their relevance in AF termination by PVI. In this study, a higher concentration of PSs in the PPVV was found in patients that fully recovered 6 months after PVI.

We have also found that rotor-related metrics may be related to the substrate state since the number of rotors per second was found to be significantly higher in patients with an unsuccessful PVI only when no duration threshold was

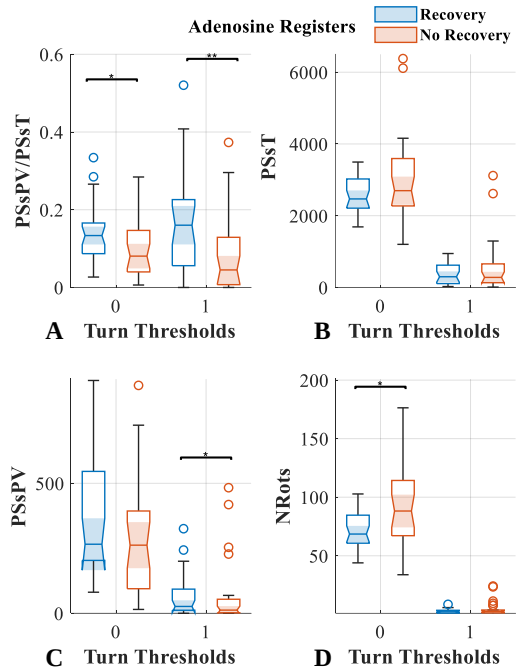

Figure 3. Rotor metrics obtained in AF patients (*p<0.05; **p<0.01): **a)** Ratio of PSs found in PPVV over PSs in the whole atria; **b)** Number of PS per second in the atria; **c)** Number of PSs in the PPVV per second; **d)** Number of rotors in the atria per second.

imposed. Podziemski et. al. stablished a relationship between PSs obtained from phase maps and spots of conduction block [3]. This relationship may provide an explanation for this last observation under the hypothesis that rotors spinning for less turns may be more frequent in conduction blocks, whereas rotors that perform more turns are more likely to be actual reentries. According to this, having many short living rotors may be due to a more diseased and complex atrial substratum.

In this study we have used atrial recordings during the infusion of adenosine so that we remove any ventricular artifact that may affect our conclusions. However, adenosine may also alter the atrial substrate and enhance driving mechanisms that may not be observable without the use of adenosine. In further studies we will investigate the ability of rotor detection in ECGI signals without adenosine infusion so that our findings can be extended to ablation planning before arrival to the EP lab.

The obtained results suggest that rotor-related metrics obtained from phase maps and ECGI contain relevant information to predict clinical outcome in PVI patients and to evaluate the state of the atrial substrate in a personalized, non-invasive way.

Acknowledgements

This work was supported by PersonalizeAF project. This project has received funding from the European Union's Horizon 2020 research and innovation program under the Marie Skłodowska-Curie grant agreement No 860974.

*This publication reflects only the author's view and that the Agency is not responsible for any use that may be made of the information it contains.

References

[1] Guillem MS, Climent AM, Rodrigo M, Fernández-Aviles F, Atienza F, Berenfeld O. Presence and stability of rotors in atrial fibrillation: Evidence and therapeutic implications. Cardiovasc Res. 2016;109(4):480–92.

[2] Li X, Almeida TP, Dastagir N, Guillem MS, Salinet J, Chu GS, et al. Standardizing Single-Frame Phase Singularity Identification Algorithms and Parameters in Phase Mapping During Human Atrial Fibrillation. Front Physiol. 2020;11(June).

[3] Podziemski P, Zeemering S, Kuklik P, van Hunnik A, Maesen B, Maessen J, et al. Rotors Detected by Phase Analysis of Filtered, Epicardial Atrial Fibrillation Electrograms Colocalize With Regions of Conduction Block. Circ Arrhythm Electrophysiol. 2018;11(10):e005858.

[4] Cluitmans M, Brooks DH, MacLeod R, Dössel O, Guillem MS, Van Dam PM, et al. Validation and opportunities of electrocardiographic imaging: From technical achievements to clinical applications. Front Physiol. 2018;9(SEP):1–19.

[5] Molero R, Climent AM, Guillem MS. Post-Processing of Electrocardiographic Imaging Signals to Identify Atrial Fibrillation Drivers. Comput Cardiol (2010). 2020;2020-Septe:2–5.

[6] Meng TW, Choi GPT, Lui LM. TEMPO: Feature-endowed teichmüller extremal mappings of point clouds. SIAM J Imaging Sci. 2016;9(4):1922–62.

[7] Bray MA, Wikswo JP. Use of topological charge to determine filament location and dynamics in a numerical model of scroll wave activity. IEEE Trans Biomed Eng. 2002;49(10):1086–93.

[8] Iyer AN, Gray RA. Experimentalist's approach to accurate localization of phase singularities during reentry. Ann Biomed Eng. 2001;29(1):47–59.

[9] Gao X, Lam AG, Bilchick KC, Darby A, Mehta N, Mason PK, et al. The use of non-invasive mapping in persistent AF to predict acute procedural outcome. J Electrocardiol [Internet]. 2019;57:S21–6. Available from: https://doi.org/10.1016/j.jelectrocard.2019.08.012

Carlos Fambuena Santos.
ITACA. Edificio 8G acceso B. Universitat Politécnica de València. Camino de Vera s/n. 46022 Valencia, Spain.
carfamsa@upvnet.upv.es